

# The Effect of Discrete Resonant Manifold Structure on Discrete Wave Turbulence

Alexander Hrabski and Yulin Pan\*

*Department of Naval Architecture and Marine Engineering,  
University of Michigan, Ann Arbor, Michigan 48109, USA*

(Dated: March 25, 2020)

We consider the long-term dynamics of nonlinear dispersive waves in a finite periodic domain. The purpose of the work is to show, for the first time, that the statistical properties of the wave field rely critically on the structure of the discrete resonant manifold (DRM). To demonstrate this, we simulate the two-dimensional MMT equation on rational and irrational tori, resulting in remarkably different power-law spectra and energy cascades at low nonlinearity levels. The difference is explained in terms of different structures of the DRM, which makes use of the recent number theory results.

## I. INTRODUCTION

Wave turbulence describes the long-term statistical behavior of a large number of dispersive waves under nonlinear interactions. For any given physical context described by nonlinear wave equations, wave turbulence theory (WTT) predicts an inertial-range power-law spectrum associated with an energy cascade process, analogous to the Kolmogorov description of hydrodynamic turbulence. Due to the generality of this mathematical framework, WTT has found wide applications including surface and internal gravity waves [e.g. 1, 2], capillary waves [e.g. 3], plasma waves [e.g. 4], acoustics [e.g. 5], and, recently, gravitational waves in the early universe [e.g. 6].

In spite of its success, WTT relies on the assumption of an infinite domain, which is violated in finite experimental facilities and numerical domains (say, with periodic boundary conditions). In these bounded systems, the spectral slope and energy flux are often observed to deviate from the WTT solutions [e.g. 7–12]. These deviations are (partly) attributed to the discreteness in wave number,  $\Delta k$ , that results from the boundary conditions of the finite domain. The effect of discreteness  $\Delta k$  on wave dynamics can be understood through the quasi-resonance conditions (say, for a quartet)

$$\begin{aligned} \mathbf{k}_1 + \mathbf{k}_2 - \mathbf{k}_3 - \mathbf{k} &= 0, \\ |\omega_{\mathbf{k}_1} + \omega_{\mathbf{k}_2} - \omega_{\mathbf{k}_3} - \omega_{\mathbf{k}}| &\leq \Omega, \end{aligned} \quad (1)$$

where  $\mathbf{k}$  represents the wave number vector and  $\omega$  is the angular frequency determined from  $\mathbf{k}$  by the dispersion relation.  $\Omega$  is the nonlinear broadening in frequency, which increases with nonlinearity level [e.g. 13, 14]. It is postulated that the WTT spectrum can only be (approximately) obtained in the regime of kinetic wave turbulence (KWT), where the nonlinear broadening overcomes the discreteness, i.e.,  $\Omega > \Delta\omega$ , with  $\Delta\omega$  as the frequency discreteness associated with  $\Delta k$ . For  $\Omega < \Delta\omega$ , the number of interacting quartets of the wave field is reduced, resulting in a deviation from the dynamics predicted by WTT.

This regime is called discrete wave turbulence (DWT), featuring clusters of interacting quartets which may constitute a cascade [15–17]. Both experiments and numerical simulations of DWT have shown, in many cases, steepened spectra compared to the KWT regime [7, 9–12], as well as restricted energy transfer (confined within small wave numbers) [8, 18] or “frozen turbulence” [7] for sufficiently small  $\Omega$ . The transition from the DWT to the KWT regime is associated with an increasing nonlinearity level which triggers a “spectral avalanche” in the corresponding “sandpile” model [19].

The traditional KWT-DWT description implies that the deviation of bounded domain dynamics from WTT depends only on the nonlinearity level and wave number discreteness. In the present work, we show that this traditional understanding overlooks a key property - the structure of the discrete resonant manifold (DRM) that survives as nonlinear broadening  $\Omega$  approaches zero, i.e., the discrete set of resonant quartets which satisfy (1) with  $\Omega = 0$ . To illustrate this idea, we conduct a numerical study of the Majda, McLaughlin, Tabak (MMT) equation [20–22] in two dimensions with dispersion relation  $\omega = |\mathbf{k}|^2$  on rational and irrational tori (periodic domains of rational and irrational aspect ratios), which correspond to different structures of DRM. We show remarkably different power-law spectra on these two tori, with the rational-torus spectral slope approaching the WTT solution with decreasing nonlinearity, in contrast to the steepened spectrum on the irrational torus (which agrees with the traditional understanding of DWT). The dynamical differences between the tori are interpreted through the different DRM structures, over which a summation of resonant interactions critically determines the energy cascade. It is found that the DRM approximates the continuous resonant manifold (CRM) of WTT (i.e., the continuous set satisfying (1) with  $\Omega = 0$ ) only on the rational torus. This can be tied to a recent number theoretic result [23], which rigorously equates the Riemann sum over the DRM of the rational torus to the integration over the CRM with a constant factor difference. We conclude by outlining the implications of our findings to general physical wave contexts.

\* yulinpan@umich.edu

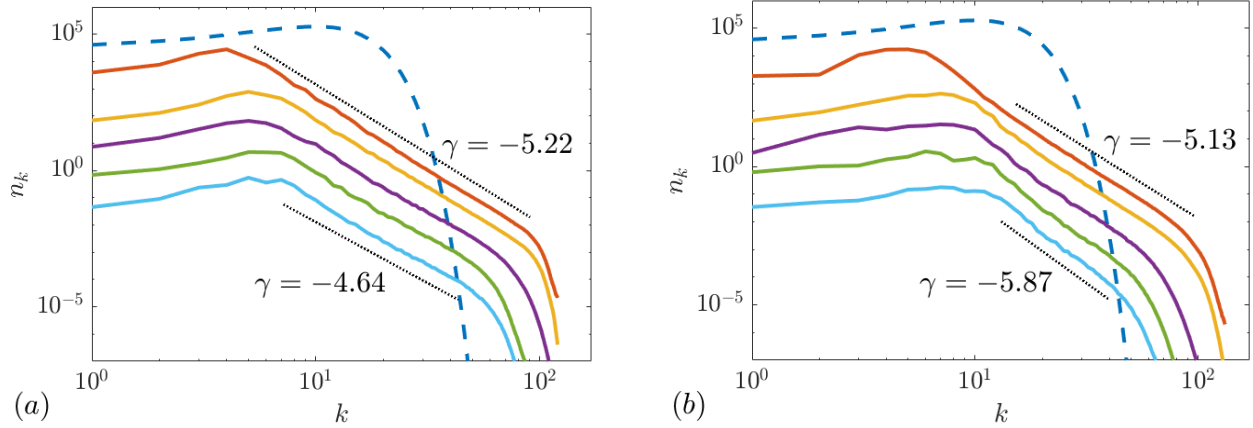


FIG. 2. The initial spectra (---) and fully-developed power-law spectra (—) calculated with  $\nu_{opt}$  at different values of  $\epsilon$  on (a)  $\mathbb{T}_r^2$  and (b)  $\mathbb{T}_{ir}^2$ . The power-law spectra are shifted for clarity, representing  $\epsilon=0.03, 0.01, 0.003, 0.001$  and  $0.0003$  from top to bottom. The linear fit for the top and bottom spectra are indicated ( $\cdot \cdot \cdot$ ).

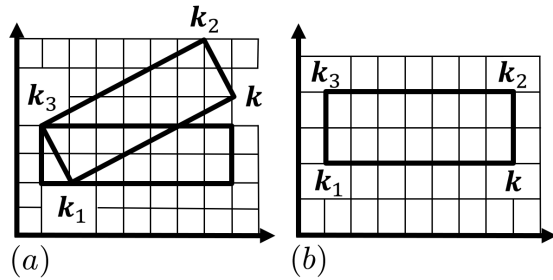


FIG. 1. Resonant quartets with  $\mathbf{k}, \mathbf{k}_1, \mathbf{k}_2$  and  $\mathbf{k}_4$  forming the four vertices of a quadrilateral (a) on  $\mathbb{T}_r^2$ , where all possible orientations on the discrete wave number grid are allowed, and (b) on  $\mathbb{T}_{ir}^2$ , where only horizontal/vertical orientations are allowed.

## II. NUMERICAL SETUP

We consider the two-parameter  $(\alpha, \beta)$  MMT equation in two spatial dimensions:

$$i \frac{\partial \psi}{\partial t} = |\partial_{\mathbf{x}}|^{\alpha} \psi + |\partial_{\mathbf{x}}|^{-\beta/4} \left( \left| |\partial_{\mathbf{x}}|^{-\beta/4} \psi \right|^2 |\partial_{\mathbf{x}}|^{-\beta/4} \psi \right), \quad (2)$$

where  $\psi \equiv \psi(\mathbf{x}, t)$  with  $\mathbf{x}$  the spatial coordinates and  $t$  the time.  $|\partial_{\mathbf{x}}|^{\alpha}$  denotes a multiplication by  $k^{\alpha}$  on each spectral component in wave number domain, with  $k = |\mathbf{k}|$ . The parameter  $\alpha = 2$  is chosen, resulting in  $\omega = k^2$ , the same dispersion relation as the nonlinear Schrödinger equation. We choose  $\beta = -4$ , which corresponds to the explosion regime of evolution [24], i.e., a fast spectral evolution with nonlinear time scale decreasing with the increase of  $k$ . The MMT equation (2) corresponds to a Hamiltonian system with the Hamiltonian  $H = H_0 + H_1$  where

$$H_0 = \int_{\mathbf{x} \in \mathbb{R}^2} \left| |\partial_{\mathbf{x}}|^{\alpha/2} \psi \right|^2 d\mathbf{x},$$

$$H_1 = \int_{\mathbf{x} \in \mathbb{R}^2} \frac{1}{2} \left| |\partial_{\mathbf{x}}|^{-\beta/4} \psi \right|^4 d\mathbf{x}. \quad (3)$$

Application of WTT on (2) (on an infinite domain) yields an analytical solution of

$$n_{\mathbf{k}} \equiv \langle \hat{\psi}_{\mathbf{k}} \overline{\hat{\psi}_{\mathbf{k}}} \rangle \sim k^{\gamma_0}, \quad (4)$$

where  $\gamma_0 = -14/3$ ,  $\hat{\psi}_{\mathbf{k}}$  is the Fourier transform of  $\psi$ ,  $\overline{\hat{\psi}_{\mathbf{k}}}$  denotes the complex conjugate of  $\hat{\psi}_{\mathbf{k}}$ , and angle brackets denote an ensemble average. This isotropic spectrum represents a stationary solution of the WTT kinetic equation [22, 25]

$$\frac{\partial n_{\mathbf{k}}}{\partial t} = \int_{(\mathbf{k}_1, \mathbf{k}_2, \mathbf{k}_3) \in \mathbb{R}^2} 4\pi k^2 k_1^2 k_2^2 k_3^2 (n_{\mathbf{k}_1} n_{\mathbf{k}_2} n_{\mathbf{k}_3} + n_{\mathbf{k}_1} n_{\mathbf{k}_2} n_{\mathbf{k}} - n_{\mathbf{k}_1} n_{\mathbf{k}_3} n_{\mathbf{k}} - n_{\mathbf{k}_2} n_{\mathbf{k}_3} n_{\mathbf{k}}) \delta(\mathbf{k}_1 + \mathbf{k}_2 - \mathbf{k}_3 - \mathbf{k}) \delta(\omega_{\mathbf{k}_1} + \omega_{\mathbf{k}_2} - \omega_{\mathbf{k}_3} - \omega_{\mathbf{k}}) d\mathbf{k}_1 d\mathbf{k}_2 d\mathbf{k}_3, \quad (5)$$

where  $\delta$  is the Dirac delta function.

In order to study the effect of DRM structure, we also consider (2) on rational and irrational tori  $\mathbb{T}_r^2$  and  $\mathbb{T}_{ir}^2$  of sizes  $2\pi \times 2\pi/q$ , with  $q = 1$  for  $\mathbb{T}_r^2$  and  $q^2 = \sqrt{2}$  for  $\mathbb{T}_{ir}^2$ . The corresponding discrete wave numbers are taken from the sets  $\mathbb{Z}_{r,ir}^2 \equiv \mathbb{Z} \times q\mathbb{Z}$ . While any irrational number  $q$  results in an irrational torus, the particular value  $q^2 = \sqrt{2}$  eliminates the majority of resonant quartets that exist in  $\mathbb{T}_r^2$ . We provide a sketch of the allowed resonant quartets on  $\mathbb{T}_r^2$  and  $\mathbb{T}_{ir}^2$  in figure 1, with theoretical justification given in [25].

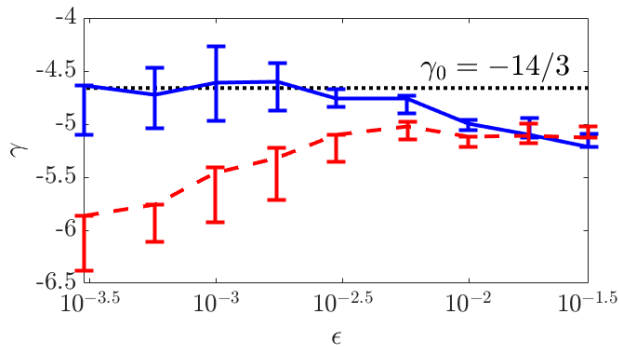


FIG. 3. Spectral slope  $\gamma$  computed using  $\nu_{opt}$  as a function of  $\epsilon$  on  $\mathbb{T}_r^2$  (—) and  $\mathbb{T}_{ir}^2$  (---). The uncertainties associated with  $\nu_R$  are shown by the vertical bars. The WTT analytical solution  $\gamma_0 = -14/3$  is indicated ( $\cdot \cdot \cdot$ ).

We simulate (2) using a GPU-accelerated pseudo-spectral method with  $170 \times 170$  alias-free modes on both  $\mathbb{T}_r^2$  and  $\mathbb{T}_{ir}^2$ . Although the irrational number  $q^2 = \sqrt{2}$  is truncated in its double-precision representation, sufficiently many digits are kept to capture its full effect on the DRM. Multiple simulations of free-decay turbulence are conducted, starting from isotropic Gaussian spectra with random phases covering a broad range of nonlinearity levels. To model damping at high wave numbers, we add a term  $-i\nu|\partial_x|^8\psi$  to the right hand side of (2). The parameter  $\nu$  takes values  $\nu_R \equiv [2.50 \times 10^{-17}, 2.50 \times 10^{-16}]$ , for which clear power-law spectra can be observed at all nonlinearity levels of interest. We further consider an optimal value  $\nu_{opt}$  (for each nonlinearity level on each torus) that corresponds to the smallest  $\nu$  in  $\nu_R$  without resulting in “bottleneck” energy accumulation at high wave numbers. In the next section, we report results for  $\nu_{opt}$  as well as uncertainty bars associated with  $\nu_R$ .

### III. RESULTS

We define the nonlinearity level of a wave field as  $\epsilon \equiv H_1/(H_0 + H_1)$ . In figure 2, the initial and fully-developed spectra  $n_k$  at different values of  $\epsilon$  obtained with  $\nu_{opt}$  are plotted for  $\mathbb{T}_r^2$  and  $\mathbb{T}_{ir}^2$ . We see that, starting from initial Gaussian spectra, the fully-developed spectra exhibit power-law forms with inertial ranges of about  $2/3 \sim 4/3$  decades depending on  $\epsilon$  on each torus. We evaluate the spectral slope  $\gamma$  based on a linear fit of the inertial power-law range (see dashed line indication in figure 2).

Figure 3 plots the spectral slope  $\gamma$  obtained with  $\nu_{opt}$  as a function of  $\epsilon$  (ranging two orders of magnitude) on both tori. We also include the uncertainty bars computed from the range  $\nu_R$ , which show insignificant impacts on the values of  $\gamma$  (with an order of magnitude variation of  $\nu$ , the largest uncertainty in  $\gamma$  is  $\mathcal{O}(0.5)$ ). At high nonlinearity levels, the values of  $\gamma$  on both tori are almost identical, and about 0.5 smaller (i.e., steeper spectra)

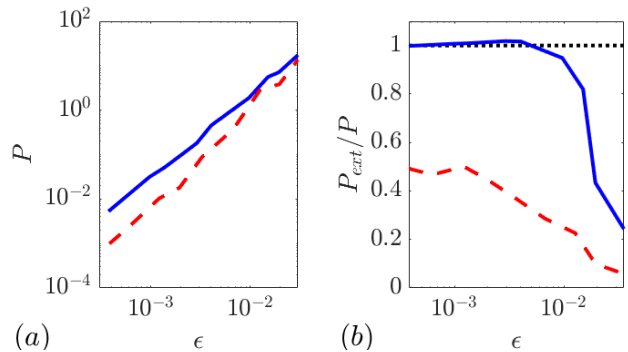


FIG. 4. (a)  $P$  and (b)  $P_{ext}/P$  as functions of  $\epsilon$  on  $\mathbb{T}_r^2$  (—) and  $\mathbb{T}_{ir}^2$  (---). The line of  $P_{ext}/P = 1$  ( $\cdot \cdot \cdot$ ) is indicated in (b).

than the WTT value  $\gamma_0 = -14/3$ . With the decrease of nonlinearity, the spectral slope  $\gamma$  exhibits remarkably different behaviors on the two tori. On  $\mathbb{T}_{ir}^2$ ,  $\gamma$  decreases with  $\epsilon$ , indicating steepened spectra in agreement with previous observations on other wave systems [7, 9–12]. However, on  $\mathbb{T}_r^2$ ,  $\gamma$  approaches and remains at  $\gamma_0$  with the decrease of  $\epsilon$ , a trend unexplained by the traditional KWT-DWT theory.

To understand the behavior of  $\gamma$ , we further investigate the energy cascade on both tori. Unlike the previous evaluation of energy flux  $P$  based on the dissipation (or energy input) rate [e.g. 9, 26–28], we develop a new approach to evaluate  $P$  directly from the dynamical equation (2), which rules out the uncertainties associated with the quasi-stationary state and the artificial form of the dissipation. The new approach also allows us to distinguish the contribution to  $P$  from exact-resonant and quasi-resonant interactions, i.e.,  $P = P_{ext} + P_{qua}$ , a key element of our analysis. From a control volume argument, we obtain

$$P_* = - \sum_{k < k_b} \omega_k \frac{\partial n_k}{\partial t} \Big|_*, \quad (6)$$

where  $*$  denotes either *ext* or *qua* (i.e., quantities associated with exact resonance or quasi-resonance), and  $k_b$  is a wave number in the inertial range. We use  $k_b = 25$  for the subsequent results and have confirmed that the choice of  $k_b$  does not affect our conclusions. The quantity  $\partial n_k / \partial t|_*$  can be directly derived from (2) [25]:

$$\frac{\partial n_k}{\partial t} \Big|_* = \sum_{(\mathbf{k}_1, \mathbf{k}_2, \mathbf{k}_3) \in S_*} 2k_1 k_2 k_3 \text{Im} \langle \hat{\psi}_{\mathbf{k}} \hat{\psi}_{\mathbf{k}_1} \hat{\psi}_{\mathbf{k}_2} \overline{\hat{\psi}_{\mathbf{k}_3}} \rangle, \quad (7)$$

for  $\mathbf{k}, \mathbf{k}_1, \mathbf{k}_2, \mathbf{k}_3 \in \mathbb{Z}_r^2$  or  $\mathbb{Z}_{ir}^2$ ,

where  $\text{Im}$  denotes the imaginary part of a function,  $S_{ext} \equiv \{(\mathbf{k}_1, \mathbf{k}_2, \mathbf{k}_3) | \mathbf{k}_1 + \mathbf{k}_2 - \mathbf{k}_3 - \mathbf{k} = 0, \omega_{\mathbf{k}_1} + \omega_{\mathbf{k}_2} - \omega_{\mathbf{k}_3} - \omega_{\mathbf{k}} = 0\}$ , and  $S_{qua} \equiv \{(\mathbf{k}_1, \mathbf{k}_2, \mathbf{k}_3) | \mathbf{k}_1 + \mathbf{k}_2 - \mathbf{k}_3 - \mathbf{k} = 0, \omega_{\mathbf{k}_1} + \omega_{\mathbf{k}_2} - \omega_{\mathbf{k}_3} - \omega_{\mathbf{k}} \neq 0\}$ .

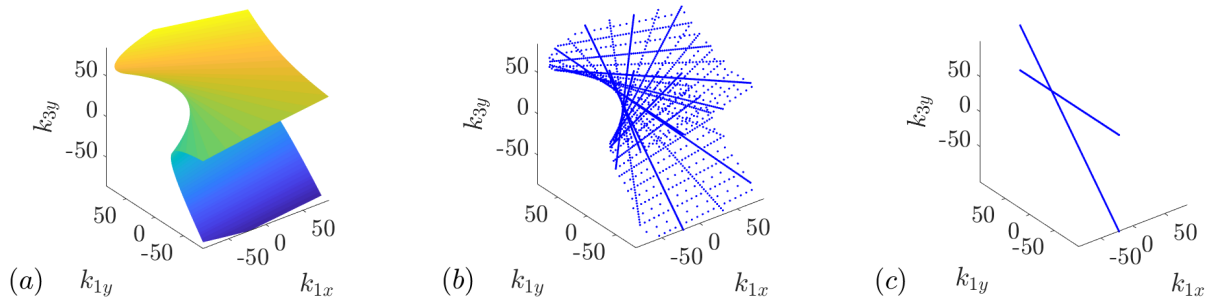


FIG. 6. (a) the CRM, (b) the DRM on  $\mathbb{T}_r^2$  and (c) the DRM on  $\mathbb{T}_{ir}^2$  for  $\mathbf{k}_2 = (-36, 31q)$  and  $k_{3x} = -22$ .

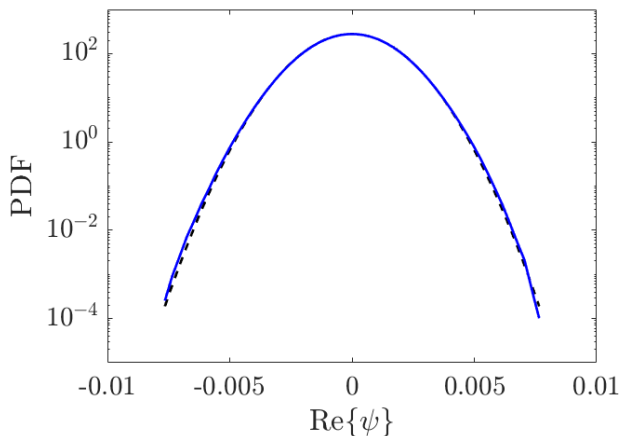


FIG. 5. Probability density function (PDF) of  $\text{Re}\{\psi\}$  (L) at  $\epsilon = 0.0003$  on  $\mathbb{T}_r^2$ , compared with the Gaussian distribution (---).

Figure 4(a) shows the total flux  $P$  as a function of  $\epsilon$  for both tori. The values of  $P$  on  $\mathbb{T}_r^2$  are consistently larger than those on  $\mathbb{T}_{ir}^2$ , with a pronounced difference (about one decade) for small  $\epsilon$ . This indicates that the energy cascade is far more efficient on  $\mathbb{T}_r^2$ , especially at low nonlinearity. We further plot  $P_{ext}/P$  as a function of  $\epsilon$  in figure 4(b). With the decrease of  $\epsilon$ , it is found that  $P_{ext}/P$  on  $\mathbb{T}_r^2$  quickly approaches unity, showing the dominance of exact resonance on the energy cascade at low nonlinearity. The regime of  $P_{ext}/P \approx 1$  occurs consistently with  $\gamma \approx \gamma_0$  for nonlinearity level  $\epsilon \lesssim 0.005$  on  $\mathbb{T}_r^2$ . On the other hand, the ratio  $P_{ext}/P$  on  $\mathbb{T}_{ir}^2$  increases much slower, not exceeding 50% in the range of nonlinearities of interest. This analysis implies that the surviving exact resonances at low nonlinearity are critical in understanding the agreement between  $\gamma$  and  $\gamma_0$  on  $\mathbb{T}_r^2$ , as well as the steepened spectrum on  $\mathbb{T}_{ir}^2$ .

#### IV. ROLE OF THE DRM

In this section, we further investigate the structure of the resonant set  $S_{ext}$ , termed the discrete resonant man-

ifold (DRM), which becomes increasingly important to the dynamics with the decrease of nonlinearity level. In particular, we will show that  $\partial n_{\mathbf{k}}/\partial t|_{ext}$  in (7) is related to the WTT kinetic equation, which explains  $\gamma = \gamma_0$  at low nonlinearity on  $\mathbb{T}_r^2$ .

It has been rigorously proven by number theory [23] that for the dispersion relation  $\omega = k^2$  on the  $\mathbb{T}_r^2$ , the summation in (7) over  $S_{ext}$  (the DRM) converges to an integral on the corresponding CRM with a factor difference in the limit of high wave numbers. Built on the *continuous resonant equation* given in [23], we can derive [25]

$$\left. \frac{\partial n_{\mathbf{k}}}{\partial t} \right|_{ext} \sim \int_{(\mathbf{k}_1, \mathbf{k}_2, \mathbf{k}_3) \in S_{ext}} 2kk_1k_2k_3 \text{Im} \langle \hat{\psi}_{\mathbf{k}} \hat{\psi}_{\mathbf{k}_1} \hat{\psi}_{\mathbf{k}_2} \hat{\psi}_{\mathbf{k}_3} \rangle d\mathbf{k}_1 d\mathbf{k}_2 d\mathbf{k}_3, \quad \text{for } \mathbf{k}, \mathbf{k}_1, \mathbf{k}_2, \mathbf{k}_3 \in \mathbb{R}^2. \quad (8)$$

At low nonlinearity,  $\partial n_{\mathbf{k}}/\partial t = \partial n_{\mathbf{k}}/\partial t|_{ext}$  on  $\mathbb{T}_r^2$ . We can then formulate the kinetic equation (5) (up to a factor difference) based on (8), under the quasi-Gaussian statistics of  $\psi$ , which we have confirmed with numerical data at low nonlinearity (figure 5). Therefore, the spectral slope on  $\mathbb{T}_r^2$  yields  $\gamma = \gamma_0$  as in the stationary solution of (5). On the other hand, (8) is not satisfied for  $\mathbb{T}_{ir}^2$ , resulting in the steepened spectra at low nonlinearity level as previously explained in the KWT-DWT framework.

We further elaborate the structure of the DRMs on  $\mathbb{T}_r^2$  and  $\mathbb{T}_{ir}^2$  using a numerical example. For visualization, we fix  $\mathbf{k}_2 = (-36, 31q)$  and  $k_{3x} = -22$ , and parameterize the set  $S_{ext} = \{k_{1x}, k_{1y}, k_{3y}\}$  by  $\mathbf{k}$ . We plot  $S_{ext} \cap \{\mathbf{k}, \mathbf{k}_1, \mathbf{k}_2, \mathbf{k}_3 \in \mathbb{R}^2\}$  (CRM),  $S_{ext} \cap \{\mathbf{k}, \mathbf{k}_1, \mathbf{k}_2, \mathbf{k}_3 \in \mathbb{T}_r^2\}$  (DRM on  $\mathbb{T}_r^2$ ) and  $S_{ext} \cap \{\mathbf{k}, \mathbf{k}_1, \mathbf{k}_2, \mathbf{k}_3 \in \mathbb{T}_{ir}^2\}$  (DRM on  $\mathbb{T}_{ir}^2$ ) in figure 6. While the DRM on  $\mathbb{T}_r^2$  resembles the CRM, the DRM on  $\mathbb{T}_{ir}^2$  is fundamentally different with a diminished number of resonant quartets. The salient contrast in these DRM structures is the inherent reason for different DWT dynamics on  $\mathbb{T}_r^2$  and  $\mathbb{T}_{ir}^2$ .

## V. CONCLUSIONS AND DISCUSSIONS

Through simulations of the 2D MMT equation (with dispersion relation  $\omega = k^2$ ) on rational and irrational tori ( $\mathbb{T}_r^2$  and  $\mathbb{T}_{ir}^2$ ), we identify the critical effect of the structure of discrete resonant manifold (DRM) on discrete wave turbulence (DWT). On  $\mathbb{T}_r^2$ , the DRM structure resembles the continuous resonant manifold (CRM), with a Riemann summation over the DRM converging to an integral over the CRM. The spectral slope thus approaches  $\gamma_0$  for low nonlinearity as predicted by the WTT kinetic equation. On  $\mathbb{T}_{ir}^2$ , the DRM is altered by the diminished number of resonant quartets, leading to steepened spectrum and reduced energy cascade capacity with the decrease of nonlinearity.

The DRM structure relies on the number-theoretic properties of  $S_{ext}$  (in particular whether (7) can be related to (8)). These properties depend on the dispersion relation, domain aspect ratio and dimensionality,

and the number of modes involved in each interaction. Therefore, different physical wave systems may have different DWT dynamics, which leads to much richer and more diverse physics than that in the unified KWT-DWT framework (e.g., capillary wave turbulence on  $\mathbb{T}_r^2$  shows steepened spectrum [9] in contrast to MMT turbulence). More number-theoretic results are also needed to establish the connection between (7) and (8) for other physical dispersion relations.

## VI. ACKNOWLEDGEMENTS

We would like to thank Professor Zaher Hani for fruitful discussions and his explanation of the number theoretic results. This research was supported in part through computational resources and services provided by Advanced Research Computing at the University of Michigan, Ann Arbor.

- 
- [1] V. E. Zakharov, J. Applied Mech. and Tech. Phys. **9**, 190 (1968).
  - [2] Y. V. Lvov, K. L. Polzin, E. G. Tabak, and N. Yokoyama, J. Phys. Ocean. **40**, 2605 (2010).
  - [3] V. E. Zakharov and N. Filonenko, J. Applied Mech. and Tech. Phys. **8**, 37 (1967).
  - [4] S. Galtier, S. V. Nazarenko, A. C. Newell, and A. Pouquet, J. Plasma Phys. **63**, 447488 (2000).
  - [5] V. S. Lvov, Y. Lvov, A. C. Newell, and V. Zakharov, Phys. Rev. E **56**, 390 (1997).
  - [6] S. Galtier and S. V. Nazarenko, Phys. Rev. Lett. **119**, 221101 (2017).
  - [7] A. Pushkarev and V. Zakharov, Physica D **135**, 98 (2000).
  - [8] Y. L'vov, S. Nazarenko, and B. Pokorni, Physica D **218**, 24 (2006).
  - [9] Y. Pan and D. K. P. Yue, Phys. Rev. Lett. **113**, 094501 (2014).
  - [10] P. Denissenko, S. Lukaschuk, and S. Nazarenko, Phys. Rev. Lett. **99**, 014501 (2007).
  - [11] R. Hassaini and N. Mordant, Phys. Rev. Fluids **3**, 094805 (2018).
  - [12] L. Deike, B. Miquel, P. Gutierrez, T. Jamin, B. Semin, M. Berhanu, E. Falcon, and F. Bonnefoy, J. Fluid Mech. **781**, 196225 (2015).
  - [13] Y. Pan and D. K. Yue, J. Fluid Mech. **816** (2017).
  - [14] V. Lvov and S. Nazarenko, Phys. Rev. E **82**, 056322 (2010).
  - [15] E. Kartashova, Physica D **46**, 43 (1990).
  - [16] E. Kartashova, Phys. Rev. Lett. **98**, 214502 (2007).
  - [17] E. Kartashova, EPL **87**, 44001 (2009).
  - [18] C. Connaughton, S. Nazarenko, and A. Pushkarev, Phys. Rev. E **63**, 046306 (2001).
  - [19] S. Nazarenko, J. Stat. Mech. **2006**, L02002 (2006).
  - [20] A. J. Majda, D. W. McLaughlin, and E. G. Tabak, J. Nonlinear Sci. **7**, 9 (1997).
  - [21] D. Cai, A. J. Majda, D. W. McLaughlin, and E. G. Tabak, Proc. Nat. Acad. Sci. **96**, 14216 (1999).
  - [22] V. Zakharov, P. Guyenne, A. Pushkarev, and F. Dias, Physica D **152**, 573 (2001).
  - [23] E. Faou, P. Germain, and Z. Hani, J. Amer. Math. Soc. **29**, 915 (2016).
  - [24] G. Falkovich and A. V. Shafarenko, J of Nonlinear Sci. **1**, 457 (1991).
  - [25] See Supplemental Material at [URL] for derivations associated with the MMT equation and the configurations of the resonant sets of rational and irrational tori.
  - [26] Y. Pan and D. K. Yue, J. Fluid Mech. **780** (2015).
  - [27] E. Falcon, C. Laroche, and S. Fauve, Phys. Rev. Lett. **98**, 094503 (2007).
  - [28] L. Deike, M. Berhanu, and E. Falcon, Phys. Rev. E **89**, 023003 (2014).

## Supplemental Material for the Paper

### “The Effect of Discrete Resonant Manifold Structure on Discrete Wave turbulence”

Alexander Hrabski and Yulin Pan

*Department of Naval Architecture and Marine Engineering,  
University of Michigan, Ann Arbor, Michigan 48109, USA*

In this document, we provide:

- I. formulations regarding the two-dimensional (2D) MMT equation, the kinetic equation, and its analytical power-law solution in an infinite domain
- II. formulations regarding energy transfer associated with the MMT equation on a torus and its connection to the continuous resonant system
- III. the configurations of the resonant quartets on  $\mathbb{T}_r^2$  and  $\mathbb{T}_{ir}^2$

#### I. MMT FORMULATIONS IN AN INFINITE DOMAIN

We start from the 2D MMT equation (parameters  $\alpha = 2$  and  $\beta = -4$ ):

$$i \frac{\partial \psi}{\partial t} = |\partial_{\mathbf{x}}|^{\alpha} \psi + |\partial_{\mathbf{x}}|^{-\beta/4} \left( \left| |\partial_{\mathbf{x}}|^{-\beta/4} \psi \right|^2 |\partial_{\mathbf{x}}|^{-\beta/4} \psi \right). \quad (1)$$

Taking the (non-unitary) Fourier transform  $\psi \rightarrow \hat{\psi}_{\mathbf{k}}$  of (1), we obtain the  $k$ -domain representation:

$$i \frac{\partial \hat{\psi}_{\mathbf{k}}}{\partial t} = k^2 \hat{\psi}_{\mathbf{k}} + \int_{\mathbf{k}_1, \mathbf{k}_2, \mathbf{k}_3 \in \mathbb{R}^2} k k_1 k_2 k_3 \hat{\psi}_{\mathbf{k}_1} \hat{\psi}_{\mathbf{k}_2} \overline{\hat{\psi}_{\mathbf{k}_3}} \delta(\mathbf{k}_1 + \mathbf{k}_2 - \mathbf{k}_3 - \mathbf{k}) d\mathbf{k}_1 d\mathbf{k}_2 d\mathbf{k}_3. \quad (2)$$

Defining  $\langle \hat{\psi}_{\mathbf{k}} \overline{\hat{\psi}_{\mathbf{k}'}} \rangle = n_{\mathbf{k}} \delta(\mathbf{k} - \mathbf{k}')$ , the evolution of  $n_{\mathbf{k}}$  can be derived (through the subtraction of (2)  $\times \overline{\hat{\psi}_{\mathbf{k}}}$  from its conjugate):

$$\frac{\partial n_{\mathbf{k}}}{\partial t} = \int_{\mathbf{k}_1, \mathbf{k}_2, \mathbf{k}_3 \in \mathbb{R}^2} 2k k_1 k_2 k_3 \text{Im} \langle \hat{\psi}_{\mathbf{k}} \overline{\hat{\psi}_{\mathbf{k}_1}} \hat{\psi}_{\mathbf{k}_2} \overline{\hat{\psi}_{\mathbf{k}_3}} \rangle \delta(\mathbf{k}_1 + \mathbf{k}_2 - \mathbf{k}_3 - \mathbf{k}) d\mathbf{k}_1 d\mathbf{k}_2 d\mathbf{k}_3. \quad (3)$$

The following derivation for the kinetic equation involves the standard procedure to relate the forth-order moment in (3) to second-order correlations through the quasi-Gaussian closure model. The detailed procedure can be found in [1–4]. Taking a large time limit of the result ((3) with second-order correlations) yields the kinetic equation:

$$\begin{aligned} \frac{\partial n_{\mathbf{k}}}{\partial t} = & \int_{\mathbf{k}_1, \mathbf{k}_2, \mathbf{k}_3 \in \mathbb{R}^2} 4\pi k^2 k_1^2 k_2^2 k_3^2 (n_{\mathbf{k}_1} n_{\mathbf{k}_2} n_{\mathbf{k}_3} + n_{\mathbf{k}_1} n_{\mathbf{k}_2} n_{\mathbf{k}} - n_{\mathbf{k}_1} n_{\mathbf{k}_3} n_{\mathbf{k}} - n_{\mathbf{k}_2} n_{\mathbf{k}_3} n_{\mathbf{k}}) \\ & \delta(\mathbf{k}_1 + \mathbf{k}_2 - \mathbf{k}_3 - \mathbf{k}) \delta(\omega_{\mathbf{k}_1} + \omega_{\mathbf{k}_2} - \omega_{\mathbf{k}_3} - \omega_{\mathbf{k}}) d\mathbf{k}_1 d\mathbf{k}_2 d\mathbf{k}_3. \end{aligned} \quad (4)$$

While a complete derivation of the Kolmogorov-Zakharov spectra (for both forward and inverse cascades) can be formulated [1, 3, 4], only the spectral slope  $\gamma_0$  for the forward cascade is of interest for our present work. The value of  $\gamma_0$  can be conveniently obtained through  $\gamma_0 = -2s/3 - d$  (for quartet resonance) [3], where  $d$  is the dimension of  $\mathbf{k}$  and  $s$  is degree of homogeneity of the interaction kernel  $V = k k_1 k_2 k_3$ . With  $d = 2$  and  $s = -\beta = 4$  (for MMT), we obtain  $\gamma_0 = -14/3$ .

## II. MMT FORMULATIONS ON A TORUS

We define the Fourier series  $\psi(\mathbf{x}) = \sum_{\mathbf{k} \in \mathbb{Z}_{r,ir}^2} \hat{\psi}_{\mathbf{k}} e^{i\mathbf{k} \cdot \mathbf{x}}$  (for simplicity, we do not distinguish  $\hat{\psi}_{\mathbf{k}}$  from the infinite domain notation), where  $\mathbb{Z}_{r,ir}^2 \equiv \mathbb{Z} \times q\mathbb{Z}$  with  $q = 1$  for  $\mathbb{T}_r^2$  and  $q^2 = \sqrt{2}$  for  $\mathbb{T}_{ir}^2$ . The wave number domain formulation of (1) then yields

$$i \frac{\partial \hat{\psi}_{\mathbf{k}}}{\partial t} = k^2 \hat{\psi}_{\mathbf{k}} + \sum_{\substack{\mathbf{k}_1, \mathbf{k}_2, \mathbf{k}_3 \in \mathbb{Z}_{r,ir}^2 \\ \mathbf{k}_1 + \mathbf{k}_2 - \mathbf{k}_3 - \mathbf{k} = 0}} k k_1 k_2 k_3 \hat{\psi}_{\mathbf{k}_1} \hat{\psi}_{\mathbf{k}_2} \overline{\hat{\psi}_{\mathbf{k}_3}}, \quad (5)$$

Defining  $S_{ext} \equiv (\{\mathbf{k}_1, \mathbf{k}_2, \mathbf{k}_3 | \mathbf{k}_1 + \mathbf{k}_2 - \mathbf{k}_3 - \mathbf{k} = 0, \omega_{\mathbf{k}_1} + \omega_{\mathbf{k}_2} - \omega_{\mathbf{k}_3} - \omega_{\mathbf{k}} = 0\})$ , and  $S_{qua} \equiv (\{\mathbf{k}_1, \mathbf{k}_2, \mathbf{k}_3 | \mathbf{k}_1 + \mathbf{k}_2 - \mathbf{k}_3 - \mathbf{k} = 0, \omega_{\mathbf{k}_1} + \omega_{\mathbf{k}_2} - \omega_{\mathbf{k}_3} - \omega_{\mathbf{k}} \neq 0\})$ , we split the summation in (5) into two terms

$$i \frac{\partial \hat{\psi}_{\mathbf{k}}}{\partial t} = k^2 \hat{\psi}_{\mathbf{k}} + \sum_{\substack{\mathbf{k}_1, \mathbf{k}_2, \mathbf{k}_3 \in \mathbb{Z}_{r,ir}^2 \\ (\mathbf{k}_1, \mathbf{k}_2, \mathbf{k}_3) \in S_{ext}}} k k_1 k_2 k_3 \hat{\psi}_{\mathbf{k}_1} \hat{\psi}_{\mathbf{k}_2} \overline{\hat{\psi}_{\mathbf{k}_3}} + \sum_{\substack{\mathbf{k}_1, \mathbf{k}_2, \mathbf{k}_3 \in \mathbb{Z}_{r,ir}^2 \\ (\mathbf{k}_1, \mathbf{k}_2, \mathbf{k}_3) \in S_{qua}}} k k_1 k_2 k_3 \hat{\psi}_{\mathbf{k}_1} \hat{\psi}_{\mathbf{k}_2} \overline{\hat{\psi}_{\mathbf{k}_3}}, \quad (6)$$

Considering  $n_{\mathbf{k}} = \langle \hat{\psi}_{\mathbf{k}} \overline{\hat{\psi}_{\mathbf{k}}} \rangle$  for the discrete case, the evolution of  $n_{\mathbf{k}}$  can be derived (through similar procedures as the infinite domain case)

$$\frac{\partial n_{\mathbf{k}}}{\partial t} = \sum_{\substack{\mathbf{k}_1, \mathbf{k}_2, \mathbf{k}_3 \in \mathbb{Z}_{r,ir}^2 \\ (\mathbf{k}_1, \mathbf{k}_2, \mathbf{k}_3) \in S_{ext}}} 2k k_1 k_2 k_3 \text{Im} \langle \overline{\hat{\psi}_{\mathbf{k}}} \hat{\psi}_{\mathbf{k}_1} \hat{\psi}_{\mathbf{k}_2} \overline{\hat{\psi}_{\mathbf{k}_3}} \rangle + \sum_{\substack{\mathbf{k}_1, \mathbf{k}_2, \mathbf{k}_3 \in \mathbb{Z}_{r,ir}^2 \\ (\mathbf{k}_1, \mathbf{k}_2, \mathbf{k}_3) \in S_{qua}}} 2k k_1 k_2 k_3 \text{Im} \langle \overline{\hat{\psi}_{\mathbf{k}}} \hat{\psi}_{\mathbf{k}_1} \hat{\psi}_{\mathbf{k}_2} \overline{\hat{\psi}_{\mathbf{k}_3}} \rangle. \quad (7)$$

It has been proved in [5] as a number theory problem that

$$\sum_{\substack{\mathbf{k}_1, \mathbf{k}_2, \mathbf{k}_3 \in \mathbb{Z}_r^2 \\ (\mathbf{k}_1, \mathbf{k}_2, \mathbf{k}_3) \in S_{ext}}} \hat{a}_{\mathbf{k}_1} \hat{a}_{\mathbf{k}_2} \overline{\hat{a}_{\mathbf{k}_3}} \sim \int_{\substack{\mathbf{k}_1, \mathbf{k}_2, \mathbf{k}_3 \in \mathbb{R}^2 \\ (\mathbf{k}_1, \mathbf{k}_2, \mathbf{k}_3) \in S_{ext}}} \hat{a}_{\mathbf{k}_1} \hat{a}_{\mathbf{k}_2} \overline{\hat{a}_{\mathbf{k}_3}} d\mathbf{k}_1 d\mathbf{k}_2 d\mathbf{k}_3, \quad (8)$$

in the limit of high wave numbers.

By setting  $\hat{a}_{\mathbf{k}} = k \hat{\psi}_{\mathbf{k}}$ , (8) can be used to replace the sums over  $S_{ext}$  in (6) and (7) on  $\mathbb{T}_r^2$  with integrals over the CRM. Under low nonlinearity, the term regarding  $S_{qua}$  in (7) approaches zero, and we arrive at

$$\frac{\partial n_{\mathbf{k}}}{\partial t} = \frac{\partial n_{\mathbf{k}}}{\partial t} \Big|_{ext} \sim \int_{\substack{\mathbf{k}_1, \mathbf{k}_2, \mathbf{k}_3 \in \mathbb{R}^2 \\ (\mathbf{k}_1, \mathbf{k}_2, \mathbf{k}_3) \in S_{ext}}} 2k k_1 k_2 k_3 \text{Im} \langle \overline{\hat{\psi}_{\mathbf{k}}} \hat{\psi}_{\mathbf{k}_1} \hat{\psi}_{\mathbf{k}_2} \overline{\hat{\psi}_{\mathbf{k}_3}} \rangle d\mathbf{k}_1 d\mathbf{k}_2 d\mathbf{k}_3, \text{ on } \mathbb{T}_r^2. \quad (9)$$

## III. RESONANT QUARTETS ON $\mathbb{T}_r^2$ AND $\mathbb{T}_{ir}^2$

We consider the exact resonance condition for a quartet:

$$\begin{aligned} \mathbf{k}_1 + \mathbf{k}_2 - \mathbf{k}_3 - \mathbf{k} &= 0, \\ \omega_{\mathbf{k}_1} + \omega_{\mathbf{k}_2} - \omega_{\mathbf{k}_3} - \omega_{\mathbf{k}} &= 0, \end{aligned} \quad (10)$$

with dispersion relation  $\omega_{\mathbf{k}} = |\mathbf{k}|^2$ . For discrete wave number  $\mathbf{k} = (n, qm)$  with  $m, n \in \mathbb{Z}$  on  $\mathbb{T}_r^2$  ( $q = 1$ ) and  $\mathbb{T}_{ir}^2$  ( $q^2 = \sqrt{2}$ ), the resonance condition (10) can be expanded as

$$n_1 + n_2 - n_3 - n = 0 \quad (11)$$

$$m_1 + m_2 - m_3 - m = 0 \quad (12)$$

$$n_1^2 + n_2^2 - n_3^2 - n^2 = -q^2 (m_1^2 + m_2^2 - m_3^2 - m^2) \quad (13)$$

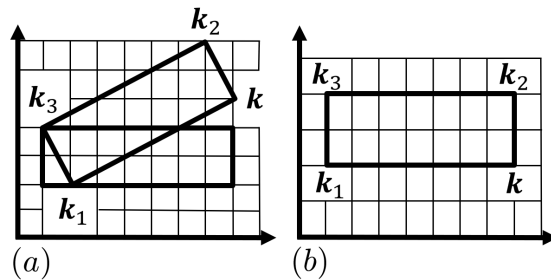


FIG. 1. Sketches of the quadrilaterals formed by vertices  $\mathbf{k}$ ,  $\mathbf{k}_1$ ,  $\mathbf{k}_2$  and  $\mathbf{k}_3$  on (a)  $\mathbb{T}_r^2$  and (b)  $\mathbb{T}_{ir}^2$ .

Substituting (11) and (12) into (13) yields

$$(n_1 - n)(n_2 - n) = -q^2(m_1 - m)(m_2 - m) \quad (14)$$

For  $\mathbb{T}_r^2$  ( $q = 1$ ), (14) is reduced to  $(\mathbf{k}_1 - \mathbf{k}) \cdot (\mathbf{k}_2 - \mathbf{k}) = 0$ , i.e.,  $(\mathbf{k}_1 - \mathbf{k}) \perp (\mathbf{k}_2 - \mathbf{k})$ . Combined with (11) and (12), it can be understood that the four vertices represented by  $\mathbf{k}$ ,  $\mathbf{k}_1$ ,  $\mathbf{k}_2$  and  $\mathbf{k}_3$  form a quadrilateral with arbitrary orientations allowed on the discrete wave number grid (figure 1(a)). For  $\mathbb{T}_{ir}^2$  ( $q^2 = \sqrt{2}$ ), (14) holds only if LHS=RHS=0, i.e.,  $n \in \{n_1, n_2\}$  and  $m \in \{m_1, m_2\}$ . Therefore, the four vertices  $\mathbf{k}$ ,  $\mathbf{k}_1$ ,  $\mathbf{k}_2$  and  $\mathbf{k}_3$  form a quadrilateral with only horizontal/vertical orientations allowed, i.e., aligned with axes (figure 1(b)).

- [1] A. J. Majda, D. W. McLaughlin, and E. G. Tabak, *J. Nonlinear Sci.* **7**, 9 (1997).
- [2] V. Zakharov, P. Guyenne, A. Pushkarev, and F. Dias, *Physica D* **152**, 573 (2001).
- [3] S. Nazarenko, *Wave Turbulence* (Springer Sci. & Bus. Media, 2011).
- [4] V. E. Zakharov, V. S. L'vov, and G. Falkovich, *Kolmogorov spectra of turbulence I: Wave turbulence* (Springer Sci. & Bus. Media, 1992).
- [5] E. Faou, P. Germain, and Z. Hani, *J. Amer. Math. Soc.* **29**, 915 (2016).